Achieving *n*-Fold Increase in the Unambiguous Radar Range of a Uniform Pulse Train by Turning Off Every *n*'th Pulse (for $n = 3, 4, 5 \dots$)

Nadav Levanon, *Life Fellow, IEEE*

Abstract— This correspondence addresses the radar challenge of extending the unambiguous delay in a uniform pulse train beyond the pulse repetition interval (PRI). The proposed approach involves dividing the streaming transmitted pulses into consecutive groups, each comprising *n* pulses. These *n* transmitted pulses undergo overlay with a coded sequence S_n (e.g., $S_3 = \{1\ 1\ 0\}$). Concurrently, the corresponding *n* reference pulses in the receiver undergo overlay with a coded sequence R_n (e.g., $R_3 = \{1\ 1\ -1\}$), requiring a sidelobe-free periodic cross-correlation between S_n and R_n. The initially identical transmitted pulses may be either plain or compressed, and the corresponding reference pulses can be matched or mismatched. This innovative approach extends the unambiguous range by a factor of *n*. However, it does not address the issue of masked target returns coinciding with detection of the system's own pulses, when the isolation of own pulses is insufficient and they saturate the receiver. Notably, the proposed approach is applicable to both coherent and non-coherent systems such as Lidar. However, our emphasis here is mainly on non-coherent systems. The presentation includes simple examples with *n* values of 3, 4, and 5, and considers system performances in the presence of noise.

Index Terms— Binary sequences, Lidar, mismatched filters, non-coherent radar, radar waveforms, range sidelobes, unambiguous range.

I. INTRODUCTION

THE unambiguous range R_{UA} of a radar transmitting a uniform pulse train is basically

$$R_{UA} = \tfrac{1}{2} C T_r \tag{1}$$

where C is the propagation velocity and T_r is the PRI. A related well known result, relevant to coherent pulse-Doppler radar [1], [2] transmiting a train of identical pulses, posits that the unamiguous Doppler is

$$\nu_{UA} = 1/T_r. \tag{2}$$

Extending the unambiguous range by increasing the PRI reduces the emitted energy per unit time, which reduces the probability of target detection. In coherent systems, this extension also brings about a reduction of the unambiguous Doppler. The widely adopted "staggered PRI" technique divides the on-target dwell time into multiple coherent processing intervals (CPI), each employing a distinct PRI [1], [2]. Staggered PRI necessiates detection in a portion of the CPIs, introducing some inefficiency in terms of both transmitted energy and detection time. Conversely, staggered PRI addresses the issue of masking by own pulses, a challenge not fully resolved by our method. Another alternative aproach is diversifying the pulse train by overlaying inter-pulse modulation or coding [3, ch.9]. In a coherent radar system, the overlaid coding can encompass phase or frequency inter-pulse coding. A crucial objective is that the periodic

overlay will exhibit perfect periodic correlation (PPC), leading to a sidelobe-free response. In certain scenarios, achieving a PPC response involves overlaying different codes - one on the transmitted pulses and another on the reference pulses, the later being numerically stored in the receiver. The two overlays need not be identical, provided their cross-correlation produces PPC [4]. A recent concept utilize pseudo-random, pulse-to-pulse, PRI staggering [5]. The distinctive feature of our proposed overlay coding is its applicability to both coherent and non-coherent systems [6], [7], [8], [9], [10].

The approach proposed here is to split the streaming identical transmitted pulses into consecutive groups, each containing *n* pulses. The *n* transmitted pulses are overlaid by an ON-OFF coded sequence S_n (*e.g.*, $S_3 = \{1\ 1\ 0\}$), and the corresponding *n* reference pulses in the receiver are overlaid by coded sequence R_n (*e.g.*, $R_3 = \{1\ 1\ -1\}$), such that the periodic cross-correlation (PCC) between S_n and R_n is perfect, namely free of sidelobes.

The simulations in this concise correspondence focus on non-coherent radar or lidar systems. However, it is important to highlight a significant implication for coherent systems. When a coherent pulse-Doppler radar processes a train of identical *p* pulses, the periodicity is T_r, and the unambiguous Doppler is as in (2). Contrastingly, when the *p* pulses are partitioned into identical groups, each group containing *n* differently coded pulses, the periodicity becomes nT_r. In a coherent system that periodicity will reduce the unambiguous Doppler to

$$\nu_{UA} = 1/(nT_r). \tag{3}$$

It should be pointed out that a field experiment [8], [9] conducted in 2008, employed a considerably more elaborate ON-OFF overlay sequence, yet succeeded in extending the unambiguous range. The experiment utilized a Furuno magnetron marine radar, which is non-coherent.

II. NON-COHERENT PULSE TRAIN

Our initial examples will use a simple train of unmodulated pulses. The most simple overlay is based on a Barker 3 sequence, where the reference sequense is $R_3 = \{1\ 1\ -1\}$ and the ON-OFF coded transmitted sequence is $S_3 = \{1\ 1\ 0\}$. The periodic cross-correlation sequence between R_3 and S_3 is $\{2\ 0\ 0\}$. The zero sidelobes indicate perfect periodic cross-correlation (PPCC). Fig. 1 shows one period of the expected noise-free and clutter-free output of the receiver processor, when there is only one target at an ambiguous delay. The top subplot shows the received own pulses (black), where pulse #3 is not emmited according to S_3. It also shows the detected target (red) at a delay longer than the PRI. The middle subplot shows the reference pulses, where the 3'rd pulse is negative, according to R_3. Recall that the processor in the receiver can use any real or complex value. The bottom subplot displays the periodic cross-correlation output, with periodicity of $3T_r$. Note the target's peak (in red) at its true delay, which is slightly longer than T_r.
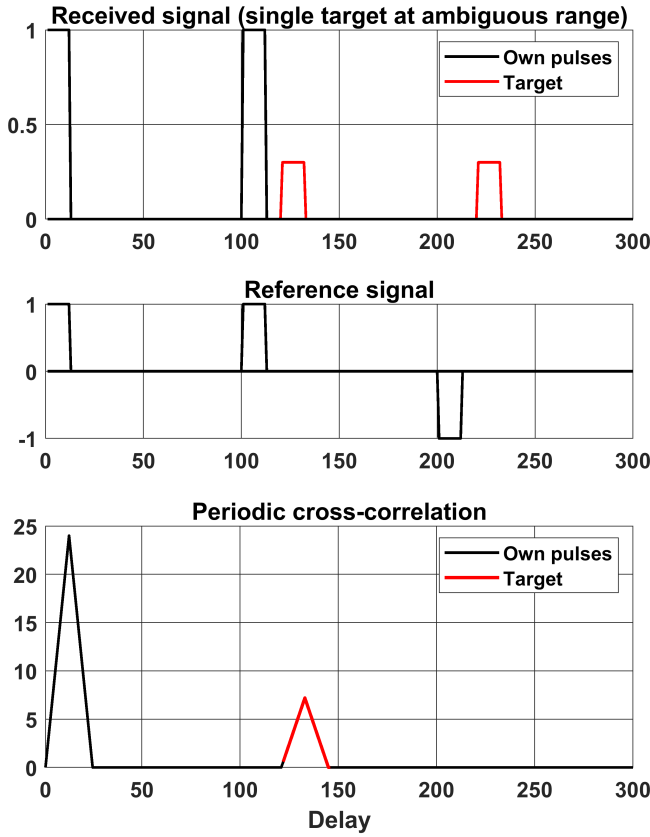
Fig. 1.   3-fold case: (top) Detected own pulses and target return at ambiguous delay, (middle) Reference pulses, (bottom) cross-correlation output. $T_r = 100$, pulse width $= 12$.

Longer unipolar sequences can be transmitted to obtain longer n-fold increases of the unambiguous range. When only one pulse is eliminated from a periodic overlay comprising n pulses, then for any $n > 2$ the sequences design rule is,

$$S_n = \{s_1 s_2 \ldots s_k \ldots s_n\}, \quad s_k = \begin{cases} 1, & k < n \\ 0, & k = n \end{cases} \qquad (4)$$

$$R_n = \{r_1 r_2 \ldots r_k \ldots r_n\}, \quad r_k = \begin{cases} 1, & k < n \\ -(n-2), & k = n \end{cases} \qquad (5)$$

The fact that the S_n and R_n sequences are different implies a mismatch. Mismatch usually entails some loss in the signal-to-noise ratio (SNR). That loss grows as the negative element of R_n grows, because when the codes are aligned that element multiplies a received element containing noise only. Similarly to Fig. 1, Fig. 2 displays the 5-fold example.

The non-coherent identical transmitted pulses in the processing interval need not be plain. The pulses can be identically intra-pulse coded, to allow pulse compresion in the receiver. However, because the receiver utilizes an envelope detector, the relevant transmitted intra-pulse coding can only be ON-OFF type, namely, utilize only two values $\{1, 0\}$. In the 3-fold, noise-free example, presented in Fig. 3, the transmitted pulses were intra-pulse coded by unipolar Barker 5 $\{1\ 1\ 1\ 0\ 1\}$. Achieving acceptable pulse compression with such a sequence requires a mismatched filter (MMF) in the receiver. The one used in Fig. 3 was $\{0.0484\ -0.4319\ -0.3714\ 0.4763\ 0.9365\ 0.4844\ -1.0576\ 0.9365\ -0.2947\ -0.3552\ 0.3552\}$ generated according to [11]. The top subplot of Fig. 3 contains
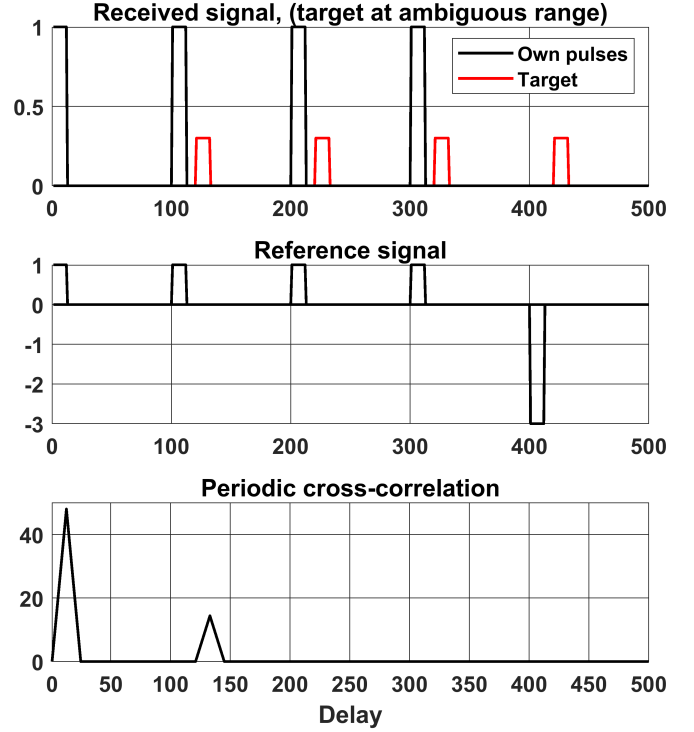
Fig. 2.   5-fold case: (top) detected own pulses and target return at ambiguous delay, (middle) reference pulses, (bottom) cross-correlation output.
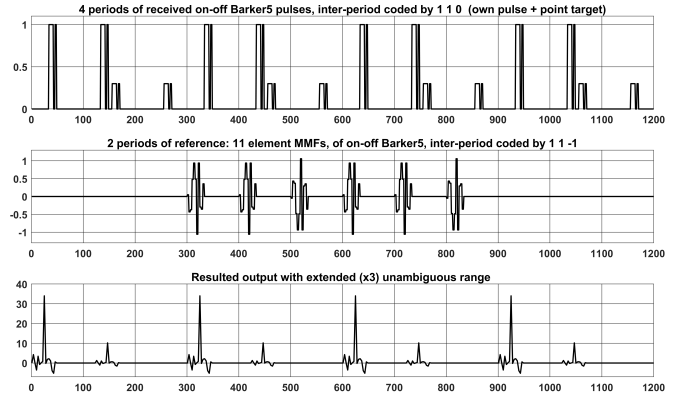
Fig. 3.   Compressed pulses: (top) received own ON-OFF pulses and returns from a point target, (middle) overlaid mismatched reference, (bottom) cross-correlation output. $T_r = 100$.

12 pulses, intra-pulse coded by unipolar Barker 5. The 12 pulses are overlaid by 3 unipolar Barker 3 sequences $\{1\ 1\ 0\}$, hence every 3'rd pulse is missing. The top subplot also shows reflection of one target at an ambiguous delay, slightly longer than one PRI. The middle subplot contains $M\ (= 2)$ consecutive groups of $n\ (= 3)$ MMFs, each group overlaid by bipolar Barker 3 sequences $\{1\ 1\ -1\}$, hence every 3'rd MMF is negated. The bottom subplot displays the resulted, noise free, periodic cross-correlation. It shows 4 periods of the 3-fold extended unambiguous delay, each containing the MMF response of the own transmitted coded pulse and of the single weaker target return. An increase in M would increase the height of the cross-correlation response.

Fig. 4 replicates Fig. 3, illustrating a scenario in which the detected target's return overlaps with the direct detection of the second pulse. It illustrates normal operation, provided that the combined signals of the two do not reach the saturation level (masking) of the receiver.
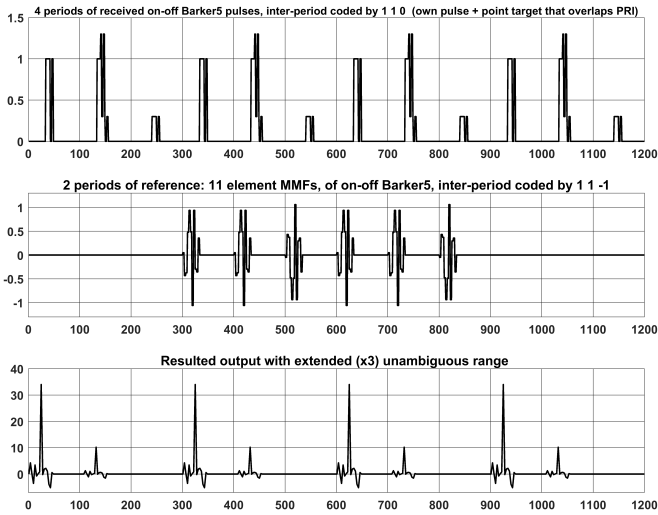
Fig. 4.   Compressed pulses. The detected point target overlaps the detected second pulse. No saturation.

The practicality of extending the unambiguous range by large factors (e.g. $n > 5$) is questionable. Should such an expansion be sought, the design rule outlined in (4) and (5) may result in extensive masking and undesirable SNR loss. An alternative approach could involve permitting the removal of multiple pulses within the transmitted periodic sequence S_n, with the stipulation that the corresponding negative elements in R_n remain constant at -1. Below is an example for $n = 7$, which appeared in [12].

$$S_7 = \{1110010\}, \quad R_7 = \{111 - 1 - 11 - 1\}.$$

The resulted periodic cross-correlation is perfect with a peak of 4, which equals the sum of the elements in S_7.

III. SUSCEPTIBILITY TO AMPLITUDE FLUCTUATIONS

Radar fluctuating targets, suitable for Doppler processing, generally belong to Swerling categories 1 or 3 [13]. In these categories fluctuations occur batch-wise rather than pulse-to-pulse. The noise-free returns from such targets maintain both amplitude and phase stability throughout the entire CPI, except for phase changes induced by Doppler shifts.

While acknowledging this property and considering its relevance in non-coherent scenarios, this section examines the impact of inter-pulse random amplitude fluctuations on the performance of the ON-OFF overlay. Specifically, a simple example will illustrate how amplitude fluctuations affect the sidelobes, demonstrating that the extended unambiguous delay remains largely free of sidelobes.

Fig. 5 displays a randomly generated case of the tops of the $p = 18$ unipolar Barker 5 pulses, used in our example, after the ON-OFF overlay removed every 3'rd pulse and after random, independent, inter-pulse amplitude fluctuations were added. The pulse amplitudes are now Gaussian distributed with mean of 1 and standard deviation of 0.03. We will assume that there were no intra-pulse fluctuations within each one of the unipolar Barker 5 coded pulses. The compression was performed by the corresponding train of identical mismatched filters, overlayed by the 3 elements binary code $\{1\ 1\ -1\}$.

Fig. 6 displays a representative cross-correlation pattern, showcasing the influence of amplitude fluctuations in the detected signal as illustrated in Fig. 5. A logarithmic scale is employed in Fig. 6 in order to highlight the exceptionally low levels of sidelobes associated with tripling the unambiguous delay from T_r to $3T_r$. The "sidelobes"
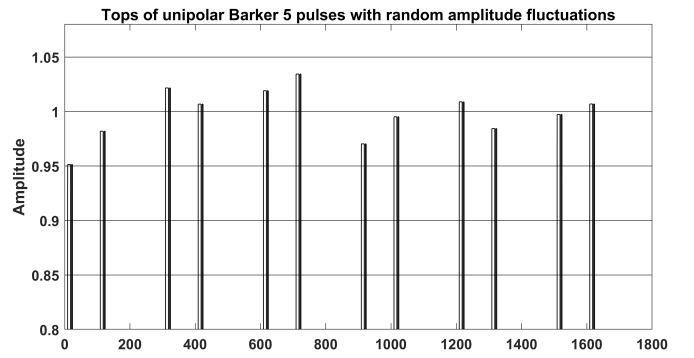
Fig. 5.   Unipolar Barker 5 pulses with random inter-pulse amplitude fluctuations.
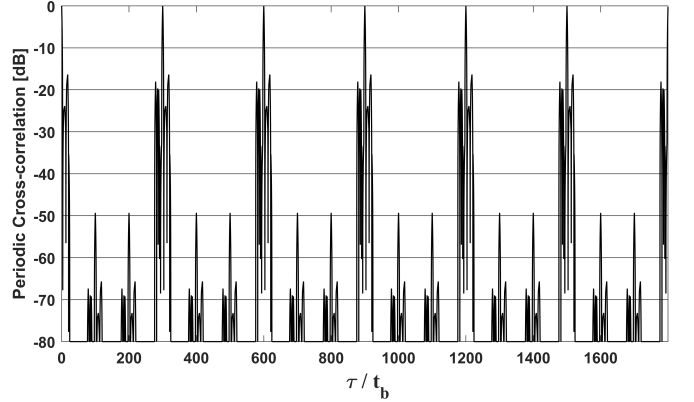
Fig. 6.   Cross-correlation between the original reference waveform and the received coded pulse train with added amplitude fluctuations. [dB scale].

manifest as approximately $-50 dB$ replicas, separated by T_r, of the main periodic responses, which themselves are spaced by $3T_r$.

IV. DETECTION IN THE PRESENCE OF NOISE

A scene similar to the one in Fig. 3 was used to simulate the nature of target detection in the presence of noise. Following an envelope detector, the additive noise is likely to exhibit a Rayleigh probability density function (PDF). A scale parameter $\sigma = 0.25$ was chosen. Recall that the noise-free target return level was $s = 0.3$ (Fig. 3, top subplot). Fig. 7 is a repeat of Fig. 3 with added noise.

The simulation detection algorithm comprised the following steps: (a) Conduct periodic cross-correlation between the streaming received signal plus noise (top subplot) and $M (= 2)$ overlaid reference periods (middle subplot). (b) Accumulate samples of the same delay, from $P (= 4)$ consecutive periods of the correlation output (bottom subplot). (c) Compare the sum of the P accumulated samples with a pre-established (or adaptive) threshold.

Presently, we encounter the classical challenge of determining an optimal threshold level to minimize the probability of false alarm (PFA) while maximizing the probability of detection (PD). This challenge is illustrated in Fig. 8, showcasing the probability density functions (PDFs) of the output sum (out_n) in the noise-only scenario (plotted in red) and the output sum (out_{s+n}) in the target with added noise scenario (plotted in black).

A notable characteristic of the noise-only scenario is the expansion of the PDFs of out_n toward exceedingly small negative values. That happens because the *inverted* MMF to unipolar Barker 5 exehbits a negative sum value,

$$- \Sigma \{0.0484, -0.4319, -0.3714, 0.4763, 0.9365, 0.4844,$$
$$-1.0576, 0.9365, -0.2947, -0.3552, 0.3552\} = -0.7265.$$
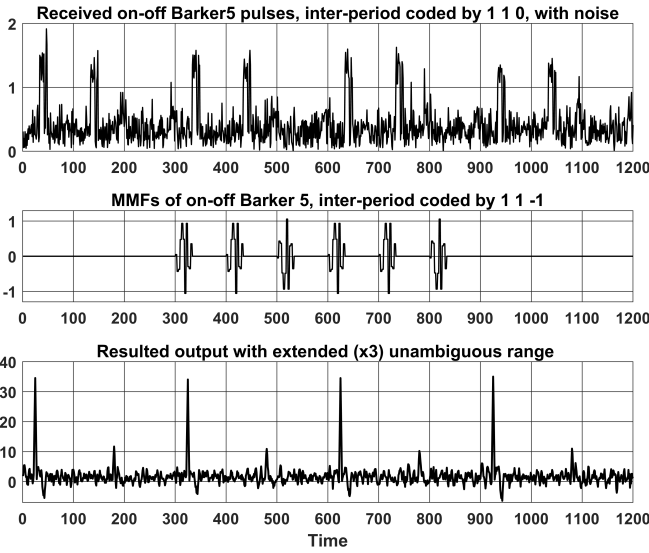
Fig. 7. Repeat of Fig. 3 with additive Rayleigh distributed noise. $T_r = 100$, $\sigma = 0.25$, $s = 0.3$.
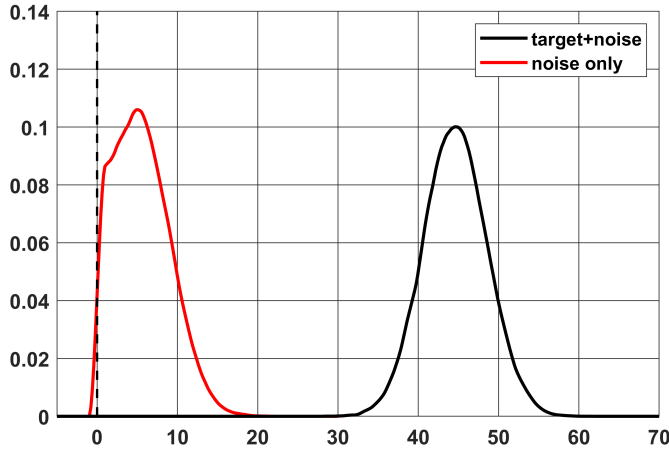
Fig. 8. PDFs of out_n and out_{s+n} for the case of: $n = 3$, $M = 2$, $P = 4$, $\sigma = 0.25$, $s = 0.3$.

Consequently, when cross-correlated with positive-only noise samples, it occasionaly yields a negative output at the sampled delay. In rare instances, this negative output may surpass the sum of M ($= 2$) values at the sampled points in the cross-correlation with the $M\text{x}(n\text{-}1)$ ($= 4$) *non-inverted* MMFs (see the negative values in the bottom subplot of Fig. 7, away from delays around the target or own pulses). Even more infrequently, the summation of P ($= 4$) samples from the same delay across P consecutive periods of the correlation output may yield a negative value.

The PDFs in Fig. 8 were produced from a Monte Carlo simulation containing 50000 runs.

V. COHERENT SCENE

Up to this point, the presented method was demonstrated on a non-coherent system. This constrained the transmitted uniform pulse train to use intra-pulse ON-OFF coding for pulse compression and inter-pulse ON-OFF coded overlay to achieve the increase in the unambiguous range. When these constrained waveforms and overlays are applied to coherent systems, the resulting correlation output remains unchanged, unless there is a Doppler shift in the target return. The impact of Doppler shift can be illustrated through the delay-Doppler response as determined by the Periodic Cross Ambiguity Function (PCAF) [14].
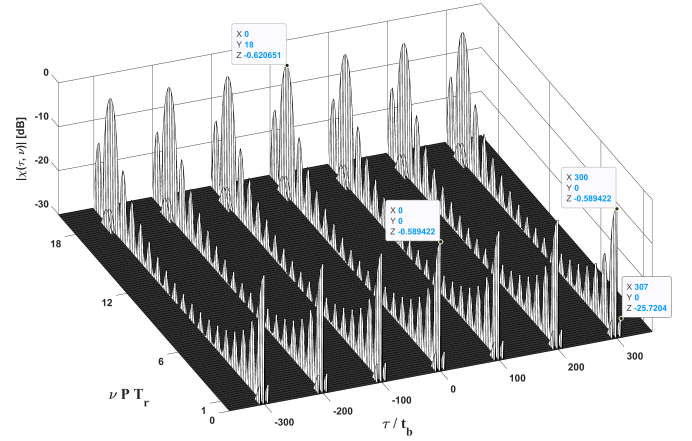
Fig. 9. Delay-Doppler response of a coherent train comprising $P = 18$ pulses, each phase coded by binary Barker 5. The receiver processing involves 11-element minISL MMFs. No inter-pulse overlay is applied.

For a more meaningful comparison between the coherent and non-coherent delay-Doppler response of the method, let's allow the coherent transmitted waveform to use phase coding. In this revised demonstration the following modifications are implemented:

(a) The ON-OFF Barker 5 intra-pulse coding {1 1 1 0 1 } is substituted with binary Barker 5 {1 1 1 −1 1 }.

(b) The 11 element mismatched filter in the receiver will be adjusted to the appropriate one for Binary Barker 5,

$$\{-0.2588 \; -0.2967 \; 0.0518 \; 0.7046 \; 1.2421 \; 0.7787$$
$$- 1.2421 \; 0.7046 \; -0.0518 \; -0.2967 \; 0.2588\}$$

(c) The 3-element phase-coded sequence {1 1 −0.5 + 0.866 j} will be overlaid on both the transmitted pulse train and on the sequence of mismatched filters in the receiver. It's worth noting that its periodic autocorrelation is {3 0 0 }.

Finally, it is well-known that the periodicity of a conventional uniform pulse train is the PRI, T_r. This leads to an unambiguous Doppler shift equal to $1/T_r$. However, when an n-element code is inter-pulse overlaid on the uniform pulse train, the periodicity increases to nT_r, thereby reducing the unambiguous Doppler shift to $1/(nT_r)$. To confirm this characteristic, the demonstration of the delay-Doppler response will commence with a PACF of a train of P uniform pulses, without any overlay.

Other pertinent parameters include: (a) t_b represents the element duration (bit). (b) The x-axis corresponds to the delay τ, normalized as τ / t_b. (c) P denotes the number of pulses in the CPI, consequently the duration of the CPI is PT_r. In the ensuing three illustrations, $P = 18$. (d) The y-axis represents the Doppler shift ν, normalized as νPT_r. By employing these normalizations, both axes become dimensionless. (e) The number of elements in the overlay is $n = 3$. (f) The z-axis represents the response using a logarithmic scale (dB).

Fig. 9 depicts the coherent scenario without overlay. At zero Doppler, a peak occurs every T_r, namely every $\tau / t_b = 100$. The peak's magnitude is -0.589 dB, reflecting the loss incurred by utilizing a MMF. The delay's peak sidelobe is also noticeable at a level of -25.7 dB. The unambiguous Doppler is evident through peaks at a normalized Doppler of $\nu PT_r = 18$. With $P = 18$, this implies that the peaks appear at $\nu = 1/T_r$, corresponding to the inverse of the PRI.

Fig. 10 illustrates the coherent scenario with phase-coded overlay. Thanks to the overlay, at zero Doppler, a peak emerges every $3T_r$, namely every $\tau / t_b = 300$. The magnitudes of the peak and of the highest sidelobe remain unchanged. However, a significant alteration
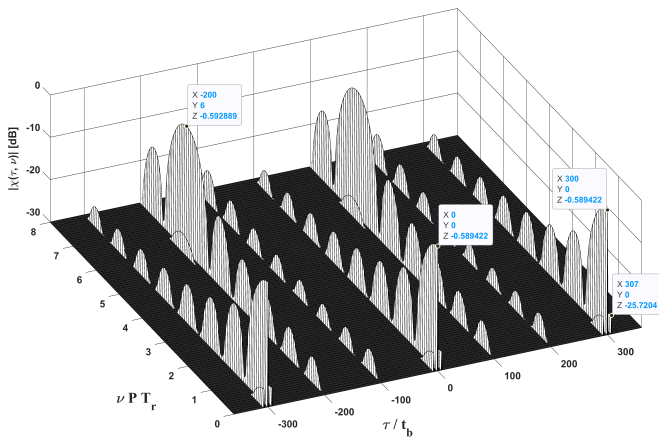
Fig. 10. Delay-Doppler response of a coherent train comprising $P = 18$ pulse, each phase coded by binary Barker 5. The receiver processing involves 11-element minISL MMFs. Phase-coded inter-pulse overlay is applied.
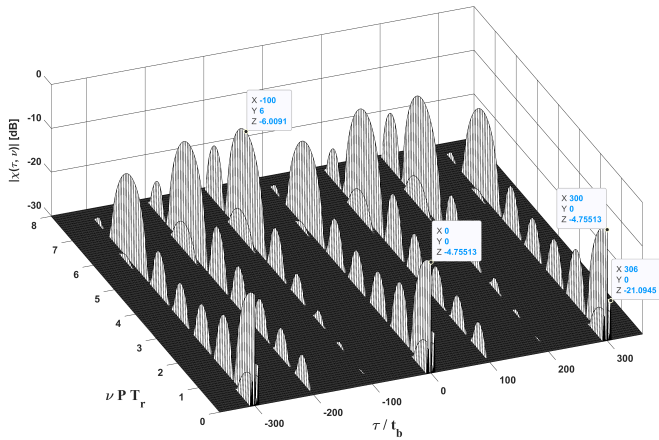
Fig. 11. Delay-Doppler response of a coherent train comprising $P = 18$ pulse, each ON-OFF coded with unipolar Barker 5. The receiver processing employs 11-element minISL MMFs. ON-OFF inter-pulse overlay is applied to the transmitted pulses.

is observed in the spacing between peaks at zero Doppler, which is now $3T_r$. Consequentially, this leads to the emergence of peaks at $\nu P T_r = 6$, signifying a reduction in the unambiguous Doppler shift to $\nu = 1/(3T_r)$.

Fig. 11 depicts a coherent scenario with an ON-OFF coded overlay, applied to the transmitted pulses {1 1 0 }, and binary overlay {1 1 −1} applied to the sequence of MMFs in the receiver. The MMFs are optimized for the unipolar Barker 5 coding of the transmitted pulses. The zero-Doppler peaks reveal a substantial loss (4.75 dB) attributed to the mismatch between the on-transmit and on-receive overlays, as well as the comparatively suboptimal performance of a MMF designed for unipolar Barker 5. This discrepancy is also accountable for the elevated near sidelobes. However, the 3-fold extension of the unambiguous range is maintained. Thanks to the symmetry property of the PCAF, it was enough to plot only its two positive Doppler quadrants.

Fig. 11 illustrates that the "turn off every n'th pulse" method is applicable to coherent systems as well, yielding the desired n-fold expansion of the unambiguous radar range. However, a comparison between Fig. 11 and Fig. 10 reveals that phase-coded overlays, exclusive to coherent systems, can achieve this task with lower loss. A concluding remark on the available phase-coded overlays: Apart from the previously mentioned 3-element overlay code, there are

suitable codes specifically at prime lengths. The 5 and 7 element phase-coded sequences are:

$$\{0.309 + 0.9511i, -0.809 + 0.5878i, 1, 1, -0.809 + 0.5878i\}$$

$$\{1, -0.75 + 0.6614i, -0.75 + 0.6614i, 1,$$

$$- 0.75 + 0.6614i, 1, 1\}.$$

VI. CONCLUSION

A novel method has been introduced to extend the unambiguous range of radar systems. This simple approach proves adaptable to both coherent and non-coherent pulse radar, along with other distance measuring sensors such as Lidar or sonar. The fundamental concept revolves around employing periodic inter-pulse ON-OFF coding overlaid onto the transmitted pulses. Simultaneously, a corresponding code is overlaid onto the reference sequence in the receiver, with no restrictions on being limited to ON-OFF values. The noise-free simulations illustrated a notable n-fold expansion in the unambiguous radar range, where n took values of 3, 4, or 5. It is worth noting that alternative sequence families have the potential to yield even greater expansion factors. Detection in the presence of noise was demonstrated on the 3-fold case by a simple simulation using an ad-hoc detection algorithm with one set of parameters. The investigation extended to the implications of applying the method in coherent systems, exploring the potential and advantages of incorporating phase-coded overlays, which are accessible in coherent systems. Future work should study detection dependence on the parameters and on noise statistics and delve into a comprehensive comparison of detection performances, particularly when contrasted with prevailing methodologies such as staggered PRI.

REFERENCES

[1] M. A. Richards, *Fundamentals of Radar Signal Processing*, 3rd ed. New York, NY, USA: MacGraw-Hill, 2022.

[2] C. Alabaster, *Pulse Doppler Radar, Principles, Technology, Applications*. New York, NY, USA: SciTech, 2012.

[3] N. Levanon and E. Mozeson, *Radar Signals*. Hoboken, NJ, USA: Wiley, 2004, doi: 10.1002/0471663085.

[4] N. Levanon, "Mitigating range ambiguity in high PRF radar using inter-pulse binary coding," *IEEE Trans. Aerosp. Electron. Syst.*, vol. 45, no. 2, pp. 687–697, Apr. 2009, doi: 10.1109/TAES.2009.5089550.

[5] R. J. Chang, C. C. Jones, J. W. Owen, and S. D. Blunt, "Gradient-based optimization of pseudo-random PRI staggering," *IEEE Trans. Radar Syst.*, vol. 1, pp. 249–263, 2023, doi: 10.1109/TRS.2023.3295808.

[6] N. Levanon, "Noncoherent pulse compression," *IEEE Trans. Aerosp. Electron. Syst.*, vol. 42, no. 2, pp. 756–765, Apr. 2006, doi: 10.1109/TAES.2006.1642589.

[7] U. Peer and N. Levanon, "Compression waveforms for non-coherent radar," in *Proc. IEEE Radar Conf.*, Apr. 2007, pp. 104–109, doi: 10.1109/RADAR.2007.374199.

[8] N. Levanon, "New waveform design for magnetron-based marine radar," *IET Radar, Sonar Navigat.*, vol. 3, no. 5, pp. 530–540, 2009, doi: 10.1049/iet-rsn.2009.0007.

[9] N. Levanon, E. Ben-Yaacov, and D. Quartler, "New waveform for magnetron marine radar—Experimental results," *IET Radar Sonar Navigat.*, vol. 6, no. 5, pp. 314–321, 2012, doi: 10.1049/iet-rsn.2011.0372.

[10] N. Levanon, I. Cohen, N. Arbel, and A. Zadok, "Non-coherent pulse compression—Aperiodic and periodic waveforms," *IET Radar, Sonar Navigat.*, vol. 10, no. 1, pp. 216–224, Jan. 2016, doi: 10.1049/iet-rsn.2015.0046.

[11] K. R. Griep, J. A. Ritcey, and J. J. Burlingame, "Poly-phase codes and optimal filters for multiple user ranging," *IEEE Trans. Aerosp. Electron. Syst.*, vol. 31, no. 2, pp. 752–767, Apr. 1995, doi: 10.1109/7.381922.

[12] S. W. Golomb, "Two-valued sequences with perfect periodic autocorrelation," *IEEE Trans. Aerosp. Electron. Syst.*, vol. 28, no. 2, pp. 383–386, Apr. 1992, doi: 10.1109/7.144563.

[13] P. Swerling, "Probability of detection for fluctuating targets," *IRE Trans. Inf. Theory*, vol. 6, no. 2, pp. 269–308, Apr. 1960, doi: 101109/TIT.1960.1057561.

[14] N. Levanon, "The periodic ambiguity function—Its validity and value," in *Proc. IEEE Radar Conf.*, Arlington, VA, USA, May 2010, pp. 204–208, doi: 10.1109/RADAR.2010.5494626.